JOURNAL OF THERMOPHYSICS AND HEAT TRANSFER
Vol. 15, No. 3, July–September 2001

Self-Consistent Model of Chemical, Vibrational, Electron Kinetics in Nozzle Expansion

G. Colonna*
National Research Council, 70126 Bari, Italy
and
M. Capitelli†
University of Bari, 70126 Bari, Italy

A self-consistent model to describe vibrational, electronically excited states (master equations) and free electron kinetics (Boltzmann equation) has been applied to study N_2 expansion through a converging–diverging conic nozzle. Strong departures from equilibrium can be observed for both vibrational, electronically excited states and electron energy distributions. In particular, the role of electronically excited states of nitrogen molecules and free electrons has been investigated. The strong interaction between these two systems, by means of inelastic and superelastic collisions, influences not only the internal state kinetics, but also the macroscopic quantities such as Mach number and gas temperature profile.

Nomenclature

A = cross-sectional nozzle area
c_p = global constant pressure specific heat
c_{ps} = molar constant pressure specific heat for sth species
c_s = speed of sound
c_{sv} = mass fraction of the sth species in vth vibrational level
E = electric field
e = electron charge
f_{sv} = energy level distributions
g_{si} = statistical weight of the ith level of the sth species
H_s^f = molar formation enthalpy for the sth species
h_i = internal enthalpy per unit mass
h_T = translational and rotational enthalpy per unit mass
J_E = contribution of electric field to the electron kinetics
J_{ee} = contribution of electron–electron collisions to the electron kinetics
J_{el} = contribution of elastic collisions to the electron kinetics
k = Boltzmann constant
M = Mach number
m = mean molar mass
m_e = electron mass
m_i = molar mass for ith species
N = total heavy particle density
n_i = mean energy distribution function value in the ith energy interval
$n(\varepsilon)$ = electron energy distribution function
P = pressure
R = universal gas constant
R_{vw} = electron–molecule rate coefficients
R^* = R/m
S_{in} = contribution of inelastic collisions to the electron kinetics
S_{sup} = contribution of superelastic collisions to the electron kinetics
S_{sv}^n = source term for molar concentration due to reaction for the continuity equation of the vth level of the sth species
S_{sv}^ρ = source term for mass density due to reaction for the continuity equation of the vth level of the sth species
T = gas temperature
T_{vs} = vibrational temperature of the sth species
u = flow speed
v, w = vibrational quantum numbers
$v(\varepsilon)$ = velocity of electrons of kinetic energy ε
x = position
α = c_p/R
α_s = c_{pi}/R for sth species
γ = c_p/c_V
ε = electron energy, eV
ε_i = mean value of the ith energy interval
ε_{ih} = upper boundary of the ith energy interval
ε_{ij}^* = threshold energy for the electron–molecule inelastic transition between $i < j$ levels
ε_{il} = lower boundary of the ith energy interval
ε_{sv} = molar energy of vth vibrational level of the sth species
$\nu(\varepsilon)$ = elastic collision frequency
$\bar{\nu}(\varepsilon)$ = mass weighted elastic collision frequency
ρ = global mass density
ρ_{sv} = mass density of the sth species in the vth vibrational level
σ_s = momentum transfer cross section for the sth species
σ_{svw} = inelastic and superelastic electron–molecule collision cross section for the transition $v \to w$ in the sth species
χ_s = molar fraction of sth species
χ_{sv} = molar fraction of sth species in the vth vibrational level

Introduction

THE role of state-to-state vibrational kinetics in nozzle flow is a topic of great interest as shown by the numerous papers appearing in the literature.[1–7] In these papers the presence of free electrons was neglected.

On the other hand, comparison with postdischarge conditions suggests that electron–molecule processes could have appreciable effects in the nozzle flow kinetics.[8] Strong nonequilibrium electron energy distribution functions (EEDF) are expected, which reflect these characteristics on the rate coefficients.[9] To study the nonequilibrium behavior of the EEDF, an appropriate Boltzmann equation for the electron kinetics must be solved.[9,10]

Strong coupling between EEDF and the molecular level distributions is present,[11] so that a self-consistent model between Boltzmann equation and heavy particle kinetics must be developed. This approach, widely used in gas discharge models,[12] is not

Received 16 November 2000; revision received 2 April 2001; accepted for publication 3 April 2001.

*Researcher, Centro di Studio per la Chimica dei Plasmi, via Orabona 4; cscpgc08@area.ba.cnr.it. Member AIAA.
†Full Professor, Chemistry Department. Member AIAA.

common in studying fluid dynamic systems. The self-consistent vibrational/electron kinetic model was applied to the boundary layer of reentry space vehicles[13] considering the concentration of electrons frozen and completely disregarding the presence of electronically excited states.

An improved model has been described by Adamovich et al.[14] for studying magnetohydrodynamics acceleration of airflows. In this case, the model, in addition to magnetohydrodynamic equations, includes chemical and ionization kinetics, vibrational level population, and metastable kinetics. An appropriate Boltzmann equation coupled with the vibrational kinetics was also considered. Apparently, the collisions from electronically excited states were neglected.

This kind of collision has been recently considered for modeling nozzle supersonic expansion[15]: In this case, however, electron density and electronically excited state concentrations were still considered frozen, and the role of the second kind collisions of electrons with excited states were parameterically taken into account.

In the present work all restrictive hypotheses have been eliminated; in particular, one mass continuity equation has been added for any electron energy value and for any electronically excited state.[11] This allows us to describe self-consistently the kinetics of electronically and vibrationally excited states and of free electrons, all of these species coupled with the one-dimensional flow equations.

Vibrational Kinetics

The model used to calculate the nozzle fluid dynamics is based on the quasi-one-dimensional steady Euler equations[3–6]

$$\frac{\mathrm{d}\rho u A}{\mathrm{d}x} = 0, \qquad \frac{\mathrm{d}P}{\mathrm{d}x} + \rho u \frac{\mathrm{d}u}{\mathrm{d}x} = 0, \qquad u\frac{\mathrm{d}u}{\mathrm{d}x} + \frac{\mathrm{d}h}{\mathrm{d}x} = 0$$

$$\frac{\mathrm{d}\rho_{sv} u A}{\mathrm{d}x} = S^{\rho}_{sv}, \qquad P = \frac{\rho RT}{m} \tag{1}$$

for reacting flows. These equations are completed by the definition of the enthalpy for nonequilibrium flows

$$h = h_T + h_i \tag{2}$$

as the sum of the translational

$$h_T = RT\frac{\sum \alpha_s \chi_s}{\sum m_s \chi_s} = \frac{\alpha RT}{m} \tag{3}$$

and internal and chemical enthalpy

$$h_i = \frac{1}{m}\left[\sum_s \chi_s\left(H_s^f + f_{sv}\varepsilon_{sv}\right)\right] \tag{4}$$

The quantity f_{sv} is the energy level distribution or the fraction of a heavy particle of the sth species in the vth level.

The chemical contribution is included in the mass continuity equation for any single species [see Eq. (1)]. The source term can be calculated from the zero-dimensional kinetic equations, obtaining the following expression for species mass fraction:

$$\frac{\mathrm{d}c_{sv}}{\mathrm{d}x} = \frac{S^{\rho}_{sv}}{\rho u A} = \frac{m_s S^{n}_{sv}}{\rho u A} \tag{5}$$

This model, as already pointed out, has been applied to study vibrational and chemical kinetics in nozzle flows. Some rearrangements are needed to extend the nozzle model when electron kinetics is coupled self-consistently with vibrational and electronic level kinetics. The procedure is schematically shown in Fig. 1.

As starting point, we consider the Boltzmann equation for free electrons in the homogeneous and almost isotropic (two terms in spherical harmonics expansion) approximation.[16] The time-dependent EEDF can be calculated by solving the equation

$$\frac{\partial n(\varepsilon)}{\partial t} = -\frac{\partial}{\partial \varepsilon}(J_E + J_{\mathrm{el}} + J_{\mathrm{ee}}) + S_{\mathrm{in}} + S_{\mathrm{sup}} \tag{6}$$

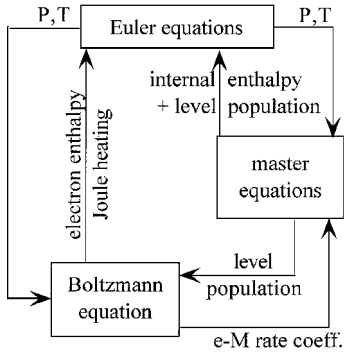

Fig. 1 Scheme of the self-consistent coupling between, heavy particle, electron kinetics, and Euler equations.

where J_E, J_{el}, and J_{ee} are the flux through electron energy axis due, respectively, to the electric field E, electron-heavy particle el, and electron–electron elastic collisions and S_{in} and S_{sup} are the source terms due to inelastic collisions,

$$\mathrm{e}^-(\varepsilon) + \mathrm{N}_2(i) \rightarrow \mathrm{e}^-(\varepsilon - \varepsilon_{ij}) + \mathrm{N}_2(j) \qquad (i < j) \tag{7}$$

and superelastic collisions,

$$\mathrm{e}^-(\varepsilon) + \mathrm{N}_2(j) \rightarrow \mathrm{e}^-(\varepsilon + \varepsilon_{ij}) + \mathrm{N}_2(i) \qquad (i < j) \tag{8}$$

The J terms depend on the derivatives (first and second) of the EEDF, whereas S terms allow the electrons to jump from one energy to another and are proportional to the EEDF. All of the terms are linear except J_{ee}, which is quadratic in the EEDF (see Ref. 16 and the Appendix for the explicit expression of J and S terms).

Writing Eq. (6) in finite difference form and considering

$$n_i = \frac{\int_{\varepsilon_{il}}^{\varepsilon_{ih}} n(\varepsilon)\,\mathrm{d}\varepsilon}{\Delta\varepsilon} \begin{cases} \varepsilon_{ih} = \varepsilon_i + 0.5\Delta\varepsilon \\ \varepsilon_{il} = \varepsilon_i + 0.5\Delta\varepsilon \end{cases} \tag{9}$$

we have in vector form[13–16]

$$\frac{\mathrm{d}\boldsymbol{n}}{\mathrm{d}t} = C\boldsymbol{n} + T(\boldsymbol{n})\boldsymbol{n} \tag{10}$$

where the nonlinear terms $\boldsymbol{T}$ are due to electron–electron coulomb collisions. Considering any energy interval as an energy (translational) level of electron, we can consider the right-hand side of Eq. (10) as the source term for electrons in Eq. (5), giving a general formulation for electron and vibrational kinetics.

The numerical approach has been widely described in previous works.[3–6] For N_2 gas, the species considered are N_2, N_2^+, N, N^+, and e^-. Only for nitrogen molecules, internal level kinetics has been taken into account, considering 45 vibrational levels and four electronically excited states

$$A^3\Sigma_u^+[\mathrm{N}_2(A)], \qquad B^3\Pi_g[\mathrm{N}_2(B)]$$
$$C^3\Pi_g[\mathrm{N}_2(C)], \qquad a'^1\Sigma_u^-[\mathrm{N}_2(a)]$$

We have used the same vibrational kinetics

$$\mathrm{N}_2(v) + \mathrm{N}_2(w) \leftrightarrow \mathrm{N}_2(v-1) + \mathrm{N}_2(w+1) \tag{11}$$

$$\mathrm{N}_2(v) + \mathrm{N}_2 \leftrightarrow \mathrm{N}_2(v-1) + \mathrm{N}_2 \tag{12}$$

$$\mathrm{N}_2(v) + \mathrm{N} \leftrightarrow \mathrm{N}_2(w) + \mathrm{N} \tag{13}$$

as well as the dissociation/recombination model (ladder climbing) used in Ref. 3–6,

$$\mathrm{N}_2(v) + \mathrm{N}_2(v') \leftrightarrow \mathrm{N}_2(v-1) + 2\mathrm{N} \tag{14}$$

$$\mathrm{N}_2(v') + \mathrm{N}_2 \leftrightarrow 2\mathrm{N} + \mathrm{N}_2 \tag{15}$$

$$\mathrm{N}_2(v) + \mathrm{N} \leftrightarrow 3\mathrm{N} \tag{16}$$

To this model we have added the kinetics of the electronically excited states

$$N_2(A) + N_2(A) \leftrightarrow N_2(B) + N_2(v = 8) \quad (17)$$

$$N_2(A) + N_2(A) \leftrightarrow N_2(C) + N_2(v = 2) \quad (18)$$

$$N_2(A) + N_2(v \geq 6) \leftrightarrow N_2(B) + N_2(v - 6) \quad (19)$$

$$N_2(A) + N \leftrightarrow N_2(v < 10) + N \quad (20)$$

$$N_2(B) \leftrightarrow N_2(A) + h\nu \quad (21)$$

$$N_2(C) \leftrightarrow N_2(B) + h\nu \quad (22)$$

$$N_2(A) + N_2 \leftrightarrow N_2(v = 0) + N_2 \quad (23)$$

$$N_2(B) + N_2 \leftrightarrow N_2(v = 0) + N_2 \quad (24)$$

$$N_2(a) + N_2 \leftrightarrow N_2(B) + N_2 \quad (25)$$

$$N_2(a) + N \leftrightarrow N_2(B) + N \quad (26)$$

$$N_2(C) + N_2 \leftrightarrow N_2(a) + N_2 \quad (27)$$

$$N + N + N_2 \leftrightarrow N_2(B) + N_2 \quad (28)$$

$$N + N + N \leftrightarrow N_2(B) + N \quad (29)$$

$$N + N + N_2 \leftrightarrow N_2(A) + N_2 \quad (30)$$

$$N + N + N \leftrightarrow N_2(A) + N \quad (31)$$

and charged species

$$N_2^+ + N \leftrightarrow N_2(v = 0) + N^+ \quad (32)$$

$$N + N \leftrightarrow N_2^+ + e^- \quad (33)$$

$$N^+ + e^- \leftrightarrow N + h\nu \quad (34)$$

$$N_2(a) + N_2(A) \leftrightarrow N_2(v = 0) + N_2^+ + e^- \quad (35)$$

$$N_2(a) + N_2(a) \leftrightarrow N_2(v = 0) + N_2^+ + e^- \quad (36)$$

$$N_2(a) + N_2(v > 24) \leftrightarrow N_2(v = 0) + N_2^+ + e^- \quad (37)$$

These processes are considered mainly in cold discharge models, and the data are quite scanty. In general, for those processes for which the analytical dependence of the rate coefficient from the temperature is unknown, the exothermal rates have been considered constant, and the rate of the reverse process is calculated applying the detailed balance principle.[3–6] In Table 1 the rate coefficients and references (see Refs. 9 and 14–19) used for processes (17–37) are reported.

This reaction scheme has been improved by adding electron–molecule (E–M) collision processes, in particular vibrational and electronic inelastic and superelastic collisions

$$e + N_2(v) \leftrightarrow N_2(w) + e \quad (38a)$$

$$e + N_2^* \leftrightarrow N_2 + e \quad (38b)$$

The rate coefficients of these processes are calculated from the EEDF. As an example, for process (38a) we have

$$R_{vw} = \int_0^\infty n(\varepsilon)\sigma_{vw}(\varepsilon)v(\varepsilon)\,d\varepsilon \quad (39)$$

The same can be written for reactive E–M processes such as dissociation and ionization. The cross sections s of these processes can be found in Refs. 20–27.

Inspection of Eq. (39) gives an idea of the strong coupling between vibrationally and electronically excited state kinetics and Boltzmann equation for EEDF: The rate coefficients of the kinetic levels depend directly on the vibrational and electronically excited state distributions, and the source terms S in Eq. (6) are proportional to the concentration level.

Table 1 Rate coefficients and references for the processes considered

Process	Rate	Reference
(17)	3.2×10^{-10} cm^3/s	9
(18)	2.6×10^{-10} cm^3/s	9
(19)	1.0×10^{-10} cm^3/s	9
(20)	5.0×10^{-11} cm^3/s	9
(21)	$1.0 \times 10^{+05}$ s^{-1}	9
(22)	$2.2 \times 10^{+05}$ s^{-1}	9
(23)	3.0×10^{-18} cm^3/s	9
(24)	3.0×10^{-11} cm^3/s	14
(25)	2.0×10^{-13} cm^3/s	15
(26)	1.0×10^{-10} cm^3/s	16
(27)	1.0×10^{-11} cm^3/s	15
(28)	2.4×10^{-33} cm^6/s	15
(29)	1.4×10^{-32} cm^6/s	15
(30)	1.7×10^{-33} cm^6/s	15
(31)	1.4×10^{-32} cm^6/s	15
(32)	$2.4 \times 10^{-15} T$, K	16, 17
(33)[a]	——	18
(34)[b]	——	19
(35)	5.0×10^{-11} cm^3/s	14
(36)	2.0×10^{-10} cm^3/s	14
(37)	6.0×10^{-14} cm^3/s	16

[a] Analytical expression is in Ref. 18.
[b] Dependence of electron temperature is in a table in Ref. 19.

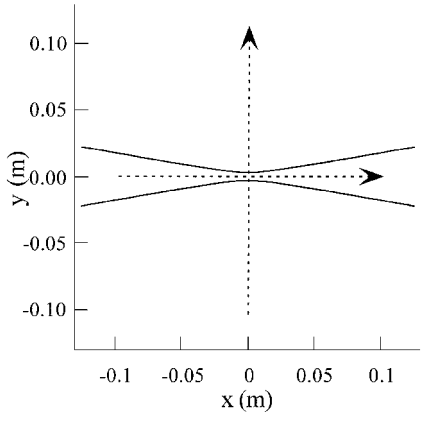

Fig. 2 Longitudinal section and reference frame of the conic nozzle.

The numerical solution of the nozzle equation for reacting flows has been widely described in Refs. 3–6. Particular care is needed in the integration of the equations because of the stiff nature of the kinetic contribution. For this reason, a step adaptive algorithm has been applied.[28] A new approach[29] to solve the Euler equations in Eq. (1) has been used to avoid the discontinuity present in the classical method.[3–6]

Note that in the present paper recombination of atomic nitrogen pumps either the ground state through the ladder climbing model or the electronically excited states through reactions (28–31).

Results and Discussion

The described model has been applied to the conic nozzle of Fig. 2 (Ref. 30). To study the role of electron kinetics on the state-to-state kinetics, we have chosen as stagnation conditions $T_0 = 10{,}000$ K and $P_0 = 1$ atm.

In previous works,[13,15] we have neglected the ionization kinetics, assuming that the molar fraction of electrons was constant along the nozzle[15] or the boundary layer.[13] This hypothesis is to a given degree confirmed by results shown in Fig. 3, where the molar fraction profiles for charged species (N^+, N_2^+, e^-) have been reported. Only the N_2^+ molar fraction changes considerably, but its fraction is too small

Table 2 Kinetic models studied and related list of considered processes

Case	Processes
a	(11–16)
b	Case a + (17–37)
c	Case b + (38)

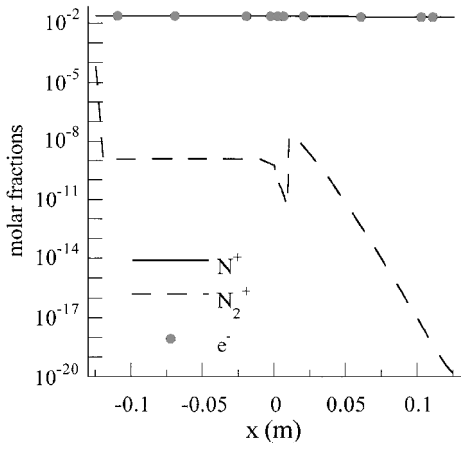

Fig. 3 Molar fraction profiles for charged species.

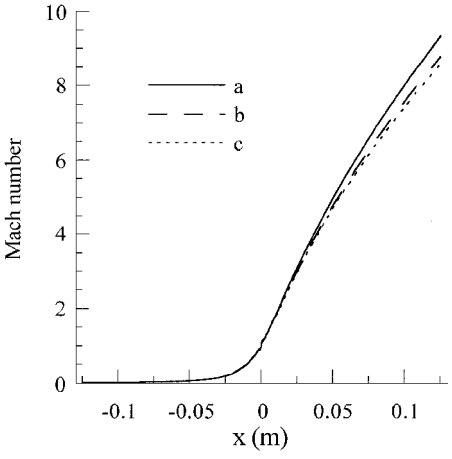

Fig. 4 Mach number profile for different kinetic schemes listed in Table 2.

to affect the ionization degree; the N^+ concentration, which determines the ionization degree, is almost constant along the nozzle axis.

To stress the importance of electronically excited state and free electron kinetics in modeling free expansion flows, we report results obtained using three different kinetic models (see Table 2). Case a describes the coupling between vibrational kinetics and Euler equations. Case b adds electronically excited state kinetics without considering E–M elementary processes. Finally, case c describes the complete kinetics (vibrational, electronically excited states, and free electron kinetics).

Macroscopic Quantities

We first analyze the role of the different kinetic schemes in affecting the macroscopic quantities such as Mach number (Fig. 4), gas temperature (Fig. 5), and vibrational and electron temperature (Fig. 6). We observe differences between the results calculated with different schemes of the order of 10% for the Mach number and 25% in the gas temperature at the nozzle outlet. Larger differences can be observed between model a (only vibrational kinetics) and model b (vibrational plus electronic excited states kinetics), whereas the differences between models b and c (complete kinetics and Boltzmann

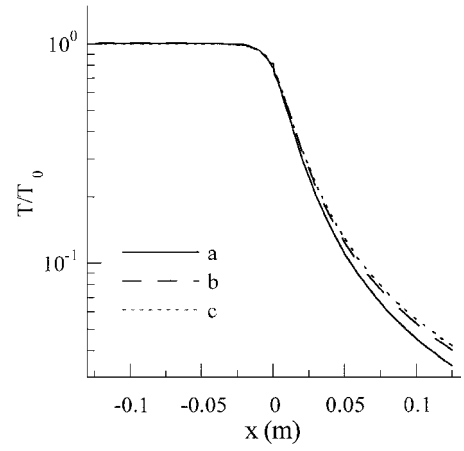

Fig. 5 Normalized gas temperature profile for different kinetic schemes listed in Table 2.

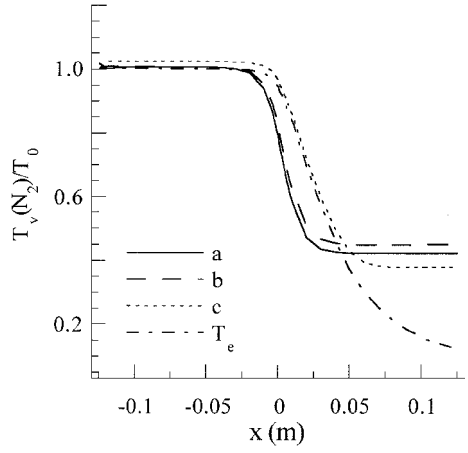

Fig. 6 Normalized vibrational temperature profiles (cases a–c) for different kinetic schemes listed in Table 2 and normalized electron temperature profile T_e in case c of Table 2.

equation for electron kinetics) are smaller. These results are important because in previous models[3–6,13,15] comparisons between isentropic (without chemical and energy level kinetics) and nonequilibrium reacting flows showed minor differences.

The vibrational temperature of nitrogen molecules decreases to equilibrate the gas temperature through vibration–translation and vibration–vibration processes [Eqs. (11–13)], but in the outlet these processes are negligible, because pressure and temperature decrease fast after the throat, and T_v reaches a constant value. The same happens to electron temperature (T_e in Fig. 6), which has the same trend of the vibrational temperature (curve c in Fig. 6) at the beginning, where electron volt processes are the most important mechanism of the low energy EEDF. However when T_v becomes constant, electron–atom (mainly) and E–M elastic processes dominate, bringing the electron temperature to lower values.

Molar Fractions

During the expansion, the molar fractions of more abundant species (e^-, N, N^+) remain almost constant (see Fig. 3), and the ionized nitrogen molecule molar fraction is too small ($<10^{-5}$) to be effective in the flow (Fig. 3). Molecular nitrogen (Fig. 7) is the only species with a sufficiently high concentration that shows appreciable variations along the nozzle axis. The cooling of the gas, due to the expansion, allows atomic recombination. A strong effect is observed when electronically excited state kinetics is considered, caused by atom recombination in $N_2(A)$ and $N_2(B)$ species [see processes (28–31)]. Electron kinetics is important in the first part of the nozzle, increasing the dissociation at high temperature and reducing the concentration of molecule.

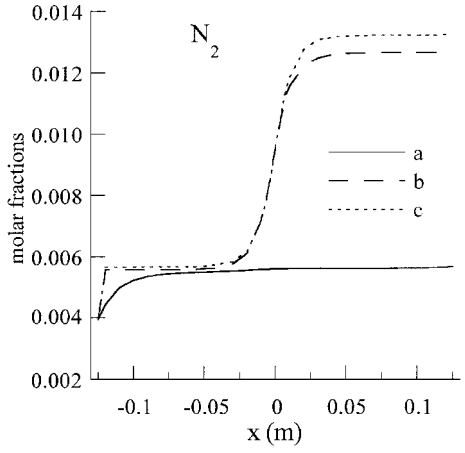

Fig. 7 N_2 molar fraction profile for different kinetic schemes listed in Table 2.

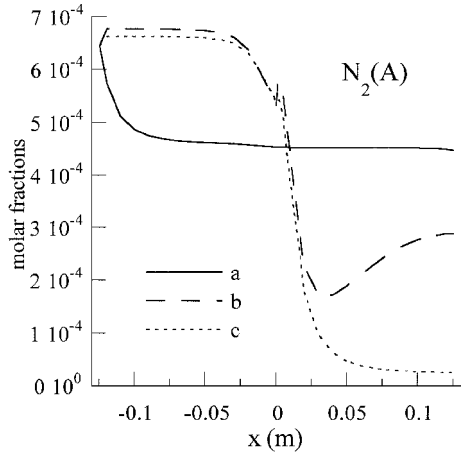

Fig. 8 $N_2(A)$ molar fraction profile for different kinetic schemes listed in Table 2.

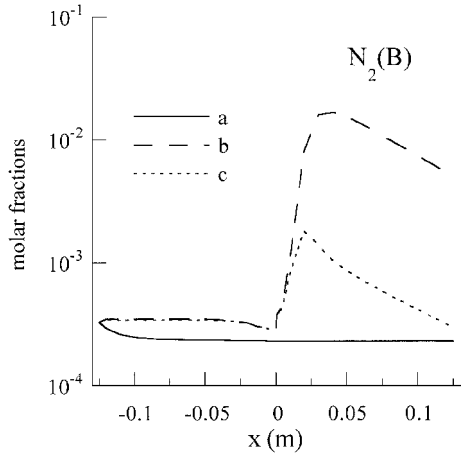

Fig. 9 $N_2(B)$ molar fraction profile for different kinetic schemes listed in Table 2.

Stronger effects can be observed in the electronically excited state concentration profiles. In Figs. 8–11, respectively, the molar fraction of levels $N_2(A)$, $N_2(B)$, $N_2(C)$, and $N_2(a')$ are reported.

In general, the presence of free electrons (case c) reduces the concentration of electronically excited states through superelastic collisions as compared with cases a and b. The only exception is represented by the profile of B state (Fig. 9). In this case, the interplay between atom recombination [process (29)] and superelastic collisions generates a peak around $x = 0.025$ m in both cases b and c: The effect of E–M collisions is to reduce the amplitude of the peak, leaving its position unchanged.

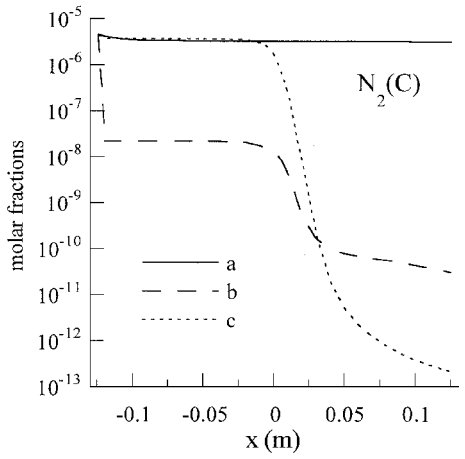

Fig. 10 $N_2(C)$ molar fraction profile for different kinetic schemes listed in Table 2.

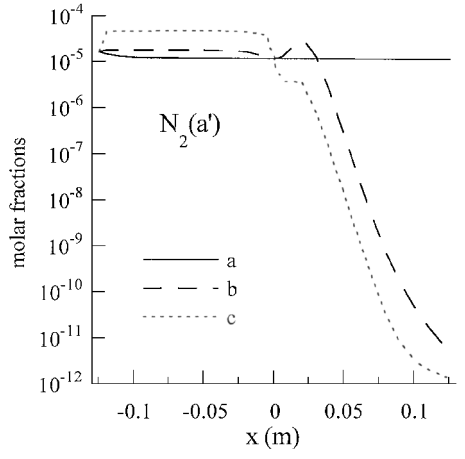

Fig. 11 $N_2(a')$ molar fraction profile for different kinetic schemes listed in Table 2.

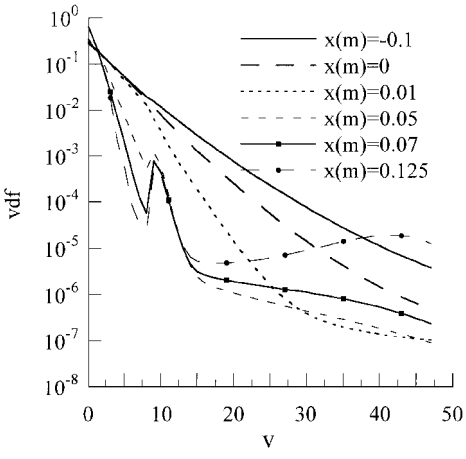

Fig. 12 VDFs, in different nozzle positions calculated in case c.

Vibrational and Electron Distributions

Because of the self-consistent coupling between chemical and kinetics level and the Boltzmann equation for free electrons, vibrational, electronic state concentrations and EEDFs are correlated. In Figs. 12 and 13 we have reported the vibrational distribution function (VDF) and EEDF in different nozzle positions for case c. Both distributions cool in the expansion following the gas temperature (see Fig. 5). In these conditions, atom recombination on the top of the vibrational ladder affects the tails of the VDF's as discussed in previous works,[3–6] electron volt superelastic processes cools the low vibrational levels, and the VDF shows a peak after the throat

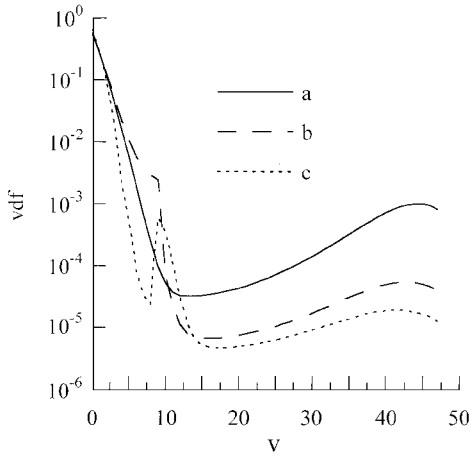

Fig. 13 VDFs, at nozzle exit calculated in the different kinetic schemes listed in Table 2.

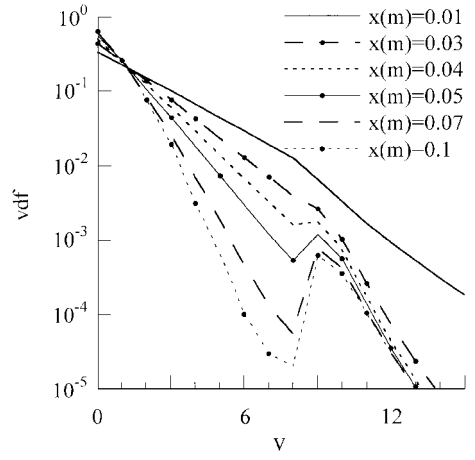

Fig. 14 Particular of the VDF peak formation in the same conditions of Fig. 12.

at $v = 10$. This effect can be attributed to electron–vibration (E–V) superelastic processes because it does not appear in the distributions calculated in cases a and b (Fig. 13). Figure 14, together with Fig. 8, can further clarify this phenomenon: At $x = 0.01$ m, we are at the maximum value of $N_2(A)$ (Fig. 8) and the VDF has a change in the slope at $v = 10$ [process (20) is very strong]. $N_2(A)$ molar fraction reduces until $x \approx 0.04$ m and the peak appears. After this point, $N_2(A)$ changes very slowly, and also the peak height is almost constant, whereas for $v < 10$, the E–V superelastic collisions prevail creating the hole in the distribution at $v = 8$.

This behavior is reflected on the electron distributions. The flux of energy from vibrational levels to electrons through E–V superelastic collisions slow down the cooling of the low energy EEDF for $x > 0.03$ m (Fig. 15). In fact, the changes in low-energy EEDF are larger for $x < 0.04$ than for $x > 0.05$. This result is confirmed also by the electron temperature profile (Fig. 6).

For $x < 0.04$ m, a plateau appears in the EEDF due to free electron superelastic collisions with $N_2(A)$ and $N_2(B)$. These distributions are very similar to postdischarge calculations.[9,10]

Elastic electron–electron (E–E) collisions are very important for the magnitude of the plateaus, as can be understood by comparing the results of Fig. 15 with that of Fig. 16, calculated by neglecting E–E collisions.

Rate Coefficients

The main consequence of the nonequilibrium electron and vibrational distributions is the strong deviation of the global rate coefficients from the Arrhenius dependence on the temperature.

When a state to state kinetics is considered, the global second-order rate coefficient of the generic reaction

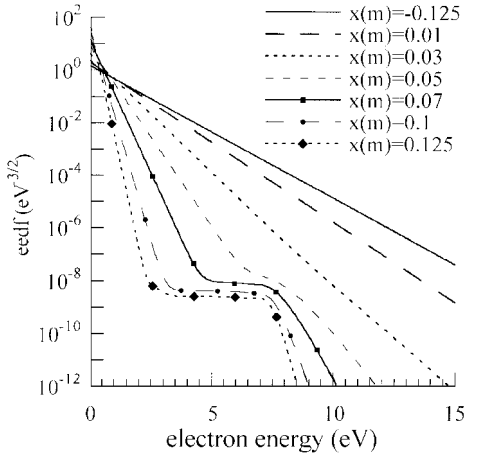

Fig. 15 EEDFs, in different nozzle positions calculated in case c.

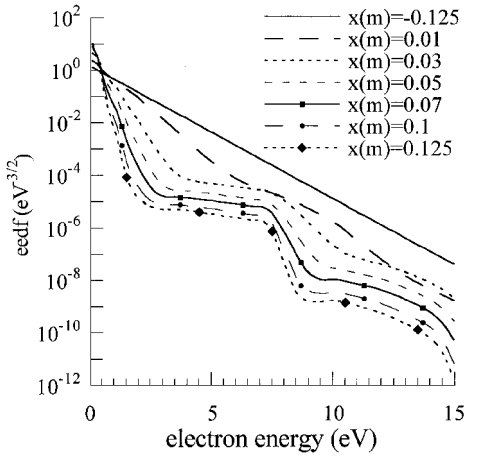

Fig. 16 EEDFs, in different nozzle positions calculated in case c neglecting elastic E–E collisions.

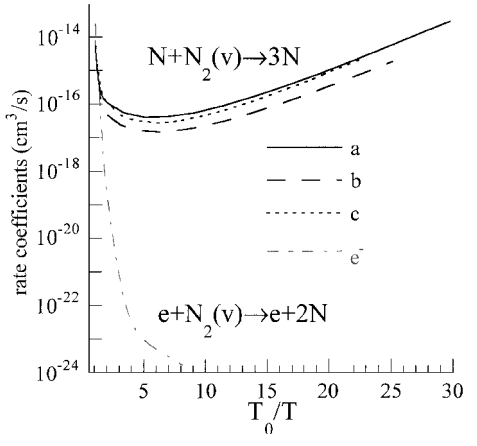

Fig. 17 Arrhenius plot of the global second-order rate coefficient of process (16) in the different models, compared with dissociation by elecron impact.

$$A + N_2(v) \xrightarrow{K_v} B + \cdots \tag{40}$$

is defined as[3–6]

$$K_g = \frac{\sum_v K_v N_2(v)}{N_2} \tag{41}$$

The Arrhenius plot of such a rate represents the dependence of the global rate as a function of the local temperature.

In Fig. 17 we show the Arrhenius plot of N_2 dissociation rate coefficient from vibrational levels by nitrogen atoms as a function of the inverse of the normalized gas temperaure and by electron impact

Table 3 Total electron impact ionization and dissociation rate coefficients (cm^3/s) compared with rate coefficients from $v = 0$ in three different nozzle positions

	$x = -0.125$		$x = 0.05$		$x = 0.125$	
	Ionization	Dissociation	Ionization	Dissociation	Ionization	Dissociation
$v = 0$	3.1×10^{-17}	5.5×10^{-16}	7.3×10^{-25}	2.0×10^{-21}	2.8×10^{-28}	8.6×10^{-25}
Total	6.9×10^{-17}	5.4×10^{-14}	1.2×10^{-24}	8.2×10^{-20}	4.2×10^{-28}	6.4×10^{-22}

Table 4 Electron impact vibrational inelastic and superelastic rate coefficients (cm^3/s) for some transition v–w and electron mean energy E and temperature T_e (K) in three different nozzle positions

	$x = -0.125$		$x = 0.05$		$x = 0.125$	
Transition	Inelastic	Superelastic	Inelastic	Superelastic	Inelastic	Superelastic
0–1	4.0×10^{-9}	6.0×10^{-9}	2.9×10^{-10}	7.7×10^{-10}	7.1×10^{-12}	6.0×10^{-11}
2–3	4.7×10^{-9}	7.1×10^{-9}	6.3×10^{-10}	1.6×10^{-9}	3.4×10^{-11}	2.0×10^{-10}
4–5	2.1×10^{-9}	3.2×10^{-9}	2.2×10^{-10}	6.0×10^{-10}	1.4×10^{-11}	8.9×10^{-11}
6–7	1.7×10^{-9}	2.6×10^{-9}	1.9×10^{-10}	5.2×10^{-10}	1.3×10^{-11}	8.1×10^{-11}
T_e	9346		3115		1881	

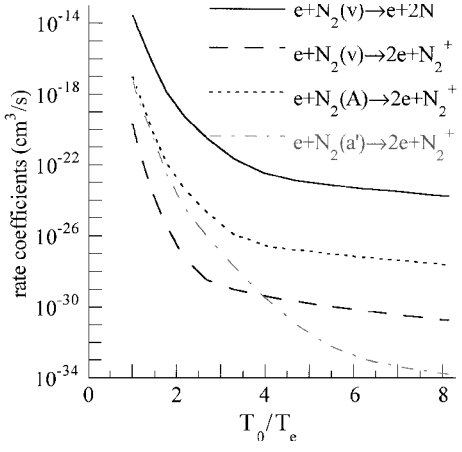

Fig. 18 Arrhenius plot of the global second-order rate coefficient of dissociation and ionization for different reactions (case c of Table 2).

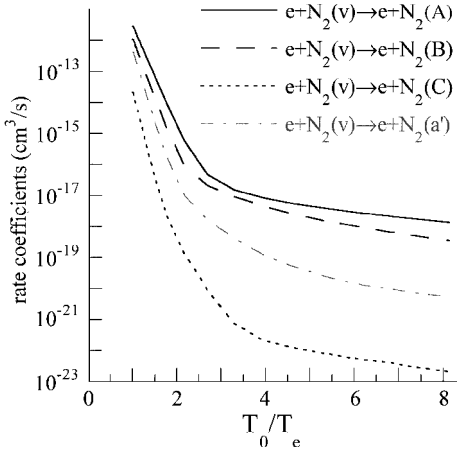

Fig. 19 Arrhenius plot of the global second-order rate coefficient of electronically excited state excitation by electron impact for different reactions (case c of Table 2).

as a function of the inverse of local electron temperature. All of the rates present non-Arrhenius trends: In some cases, the rates increase by decreasing the relevant temperature. This phenomenon has been also observed in previous works[3–6] without electronically excited states and free electron kinetics. In Fig. 18, we have plotted the E–M ionization rates from vibrational and electronically excited states compared to the global dissociation rates, in case c. The ionization rates follow the trend of the dissociation rates being in any case order of magnitudes smaller.

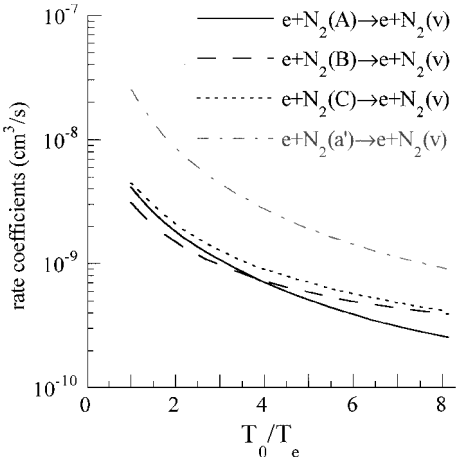

Fig. 20 Arrhenius plot of the global second-order rate coefficient of electronically excited state deexcitation by electron impact for different reactions (case c of Table 2).

In Figs. 19 and 20 we show the global rate coefficients of the excitation and quenching of electronic excited states by electron impact. The inelastic processes (Fig. 18) present strong deviations from the Arrhenius form at low temperature. This is due to the formation of the plateau in the EEDFs (see Fig. 15) for $x > 0.05$ m from the nozzle throat as well as for the corresponding plateau in the vibrational distribution functions.

Finally, we report in Tables 3 and 4 some rate coefficients for different processes at different nozzle positions. In particular Table 3 reports inelastic and superelastic electron–vibration energy exchange monoquantum rates for different initial v, whereas Table 4 compares the total ionization and dissociation rates with the corresponding values from $v = 0$.

Conclusions

The strong influence of the nonequilibrium vibrational and electronic kinetics in affecting high-enthalpy nozzle flow has been widely investigated showing important effects in chemical kinetics and rate coefficients. We have extended the model to study the role of electron kinetics and electronically excited states. These two aspects cannot be treated separately because superelastic collisions of free electrons with electronically excited states are very effective inasmuch as they can strongly affect the electron distributions for energies higher than 3 eV. The effects of the complete kinetics concern also the macroscopic quantities such as the gas temperature profile.

The model can be extended to plasma jets, introducing the electric field in the electron kinetics. This improvement is not trivial

because the heating of the gas due to joule effect should be taken into account for electrons and ions. This point has been recently analyzed, as already mentioned, by Adamovich et al.[14] for describing magnetohydrodynamics accelerators of airflows. A comparison of the present results with those reported in Ref. 14 is difficult because of the different systems treated (nitrogen against air), as well as the large differences in the considered initial ionization degree (10^{-2} against 10^{-5}).

As a conclusion, we can say that strong effects must be expected in the coupling of plasma kinetics and fluid dynamics. The present results can be further improved at every stage of the calculation, in particular in the cross sections and rate coefficients. Quantitative changes of the results should leave unchanged the qualitative features reported in this paper.

Appendix

To describe the influence of each contribution on the electron energy distributions here, we give the expression of the flux and source terms of the Boltzmann equations for the electron kinetics in Eq. (6). This equation is obtained from the general Boltzmann equation under the hypothesis that the distribution is quasi isotropic. In this case, the distribution is considered as the sum of the first two terms in the spherical harmonic expansion. The flux terms are due to electric field

$$J_E = \frac{2eE^2}{3m_e\nu(\varepsilon)}\left(\frac{n(\varepsilon)}{2} - \varepsilon\frac{\partial n(\varepsilon)}{\partial\varepsilon}\right) \tag{A1}$$

electron–atom/molecule elastic collisions

$$J_{\mathrm{el}} = \bar{\nu}(\varepsilon)\left[\left(\frac{kT}{2} - \varepsilon\right)n(\varepsilon) - kT\,\varepsilon\frac{\partial n(\varepsilon)}{\partial\varepsilon}\right] \tag{A2}$$

and to E–E collisions

$$J_{\mathrm{ee}} = \alpha\left[P(\varepsilon)\left(\frac{n(\varepsilon)}{2\varepsilon} - \frac{\partial n(\varepsilon)}{\partial\varepsilon}\right) - Q(\varepsilon)n(\varepsilon)\right] \tag{A3}$$

where

$$\nu(\varepsilon) = N\sqrt{\left(\frac{2e\varepsilon}{m_e}\right)}\sum_s \chi_s\sigma_s(\varepsilon)$$

$$\bar{\nu}(\varepsilon) = 2m_eN\sqrt{\left(\frac{2e\varepsilon}{m_e}\right)}\sum_s \frac{\chi_s\sigma_s(\varepsilon)}{m_i} \tag{A4}$$

and

$$P(\varepsilon) = \frac{2}{\sqrt{\varepsilon}}\int_0^{\varepsilon} z n(z)\,\mathrm{d}z + 2\varepsilon\int_{\varepsilon}^{\infty}\frac{n(z)}{\sqrt{z}}\,\mathrm{d}z$$

$$Q(\varepsilon) = \frac{3}{\sqrt{\varepsilon}}\int_0^{\varepsilon} n(z)\,\mathrm{d}z \tag{A5}$$

The source terms, due to jumps of electrons in the energy space, take into account inelastic collision,

$$S_{\mathrm{in}} = N\sum_{svw}\chi_{sv}[v(\varepsilon+\varepsilon_{vw})\sigma_{svw}(\varepsilon+\varepsilon_{vw})n(\varepsilon+\varepsilon_{vw}) - v(\varepsilon)\sigma_{svw}(\varepsilon)n(\varepsilon)] \tag{A6}$$

and superelastic collisions,

$$S_{\mathrm{sup}} = N\sum_{svw}\chi_{sw}[v(\varepsilon-\varepsilon_{vw})\sigma_{svw}(\varepsilon-\varepsilon_{vw})n(\varepsilon-\varepsilon_{vw}) - v(\varepsilon)\sigma_{svw}(\varepsilon)n(\varepsilon)] \tag{A7}$$

Equations (A6) and (A7) are calculated for the case $\varepsilon_{vw} = \varepsilon_w - \varepsilon_v > 0$, and the cross section for superelastic processes σ_{swv} is calculated using the microscopic reversibility

$$\sigma_{swv}(\varepsilon) = (g_{sv}/g_{sw})[(\varepsilon+\varepsilon_{vw})/\varepsilon]\sigma_{svw}(\varepsilon+\varepsilon_{vw}) \tag{A8}$$

Inelastic and superelastic collisions are the link between state-to-state and free electron kinetics.

Acknowledgments

The present paper has been partially supported by Agenzia Spaziale Italiana, MURST (under Project 9903102919-004), and INTAS (under project 99-00464).

References

[1]Kewley, D. J., "Numerical Study of Anharmonic Diatomic Relaxation Rates in Shock Waves and Nozzles," *Journal of Physics B: Molecular Physics*, Vol. 8, No. 15, 1975, pp. 2564–2579.

[2]Chiroux de Gavelle de Roany, A., Flament, C., Rich, J. W., Subramaniam, V. V., and Warren, W. R., "Strong Vibrational Nonequilibrium in Supersonic Nozzle Flows," *AIAA Journal*, Vol. 31, No. 3, 1993, pp. 119–128.

[3]Colonna, G., Tuttafesta, M., Capitelli, M., and Giordano, D., "Non-Arrhenius NO Formation Rates in One-Dimensional Nozzle Airflow," *Journal of Thermophysics and Heat Transfer*, Vol. 13, No. 3, 1999, pp. 372–375.

[4]Colonna, G., Tuttafesta, M., Capitelli, M., and Giordano, D., "NO Formation in One Dimensional Nozzle Air Flow with State-to-State Vibrational Kinetics: The Influence of $O_2(v) + N = NO + O$ Reaction," AIAA Paper 99-3685, June 1999.

[5]Colonna, G., Tuttafesta, M., Capitelli, M., and Giordano, D., "Influence of $O_2(v) + N = NO + O$ on NO Formation in One-Dimensional Air Nozzle Flow," *Journal of Thermophysics and Heat Transfer*, Vol. 14, No. 3, 2000, pp. 455, 456.

[6]Colonna, G., Tuttafesta, M., Capitelli, M., and Giordano, D., "Influence on Dissociation Rates of the State-to-State Vibrational Kinetics of Nitrogen in Nozzle Expansion," *21st Symposium on Rarefied Gas Dynamics*, Vol. 2, edited by R. Brun et al., 1998, pp. 281–288.

[7]Joshula, E., "Computational Study of Effect of Oxygen Atoms on Vibrational Relaxation of N_2 in High Speed Air Flow Past Blunt Body," AIAA Paper 99-4835, Nov. 1999.

[8]Capitelli, M., Armenise, I., Colonna, G., Giordano, D., Gorse, C., and Longo, S., "Nonequilibrium Vibrational Kinetics Under Discharge and Hypersonic Flow Conditions: A Comparison," AIAA Paper 97-2528, June 1997.

[9]Capriati, G., Colonna, G., Gorse, C., and Capitelli, M., "A Parametric Study of Electron Energy Distribution Functions and Rate and Transport Coefficients in Non Equilibrium Helium Plasmas," *Plasma Chemistry and Plasma Processing*, Vol. 12, No. 3, 1992, pp. 237–260.

[10]Colonna, G., Gorse, C., Capitelli, M., Winkler, R., and Wilhelm, J., "The Influence of Electron–Electron Collisions on Electron Energy Distribution Functions in N_2 Post Discharge Conditions," *Chemical Physics Letters*, Vol. 213, No. 1, 1993, pp. 5–9.

[11]Gorse, C., and Capitelli, M., "Coupled Electron and Excited-State Kinetics in a Nitrogen Afterglow," *Journal of Applied Physics*, Vol. 62, No. 10, 1987, pp. 4072–4076.

[12]Capitelli, M., and Gorse, C., "Non Equilibrium Plasma Kinetics," *Nonequilibrium Processes in Partially Ionized Gases*, edited by M. Capitelli and N. Bardsley, Plenum, New York, 1990, pp. 45–63.

[13]Colonna, G., and Capitelli, M., "Electron and Vibrational Kinetics in the Boundary Layer of Hypersonic Flow," *Journal of Thermophysics and Heat Transfer*, Vol. 10, No. 3, 1996, pp. 406–412.

[14]Adamovich, I. V., Rich, J. W., and Nelson, G. L., "Feasibility of Magnetohydrodynamics Acceleration of Unseeded and Seeded Airflows," *AIAA Journal*, Vol. 36, No. 4, 1998, pp. 590–597.

[15]Colonna, G., Armenise, I., Catella, M., and Capitelli, M., "Non Equilibrium Effects in Plasma Expansion Flows," *Journal of Technical Physics*, Vol. 41, No. 1, 2000, pp. 203–214.

[16]Rockwood, S. D., "Elastic and Inelastic Cross Sections for Electron-Hg Scattering from Hg Transport Data," *Physical Review A: General Physics*, Vol. 8, No. 5, 1973, pp. 2348–2358.

[17]Garscadden, A., and Nagpal, R., "Non-Equilibrium Electronic and Vibrational Kinetics in H_2–N_2 and H_2 Discharges," *Plasma Sources Science and Technology*, Vol. 4, No. 2, 1995, pp. 268–280.

[18]Gordiets, B., Ferreira, C. M., Pinheiro, M. J., and Ricard, A., "Self-Consistent Kinetic Model of Low-Pressure N_2–H_2 Discharges: I. Volume Processes," *Plasma Sources Science and Technology*, Vol. 7, No. 3, 1992, pp. 363–368.

[19]Kossyi, I. A., Kostinsky, Y. A., Matveyev, A. A., and Silakov, V. P., "Kinetic Scheme of the Non-Equilibrium Discharge in Nitrogen–Oxigen Mixtures," *Plasma Sources Science and Technology*, Vol. 1, No. 3, 1995, pp. 207–220.

[20]Cacciatore, M., Capitelli, M., and Gorse, C., "Non-Equilibrium Dissociation and Ionization of Nitrogen in Electrical Discharges: The Role of Electronic Collisions from Vibrationally Excited Molecules," *Chemical Physics*, Vol. 66, No. 1–2, 1982, pp. 141–151.

[21]Capitelli, M., and Celiberto, R., "Electron–Molecule Cross Sections for Plasma Applications: The Role of Internal Energy of the Target," *Novel Aspects of Electron–Molecule Collisions*, edited by K. H. Becker, World Scientific, Singapore, 1998, pp. 283–323.

[22]Huo, W. M., Gibson, T. L., Lima, M. A. P., and McCoy, V., "Schwinger Multichannel Study of the $^2\Pi_g$ Shape Resonance in N_2," *Physical Review A: General Physics*, Vol. 36, No. 4, 1987, pp. 1632–1641.

[23]Phelps, A. V., and Pitchford, L. C., "Anisotropic Scttering of Electrons by N_2 and Its Effects on Electron Transport: Tabulation of Cross Sections and Results," JILA Rept. 23, Univ. of Colorado, Boulder, CO, 1985.

[24]Allan, M., "Excitation of Vibrational Levels up to $v = 17$ in N_2 by Electron Impact in the 0–5 eV Region," *Journal of Physics B: Atomic and Molecular Physics*, Vol. 18, No. 22, 1985, pp. 4511–4517.

[25]Morgan, L. A., "Resonant Vibrational Excitation of N2 by Low-Energy Electron Impact," *Journal of Physics B: Atomic and Molecular Physics*, Vol. 19, No. 11, 1986, pp. L439–L445.

[26]Ton-That, D., and Flannery, M. R., "Cross Sections for Ionization Of Metastable Rare-Gas Atoms (Ne^*, Ar^*, Kr^*, Xe^*) and of Metastable N_2^*, CO^* by Electron Impact," *Physical Review A: General Physics*, Vol. 15, No. 2, 1977, pp. 517–526.

[27]Dubé, L., and Herzenberg, A., "Absolute Cross Sections from the 'Boomerang Model' for Resonant Electron–Molecule Scattering," *Physical Review A: General Physics*, Vol. 20, No. 1, 1979, pp. 194–213.

[28]Colonna, G., "Step Adaptive Method for Vibrational Kinetics and Other Initial Value Problems," *Rendiconti del Circolo Matematico di Palermo, Serie II Supplemento*, Vol. 57, 1998, pp. 159–163.

[29]Colonna, G., Tuttafesta, M., and Giordano, D., "Numerical Methods to Solve Euler Equations in One-Dimensional Steady Nozzle Flow," *Computer Physics Communications* (to be published).

[30]Shizgal, B. D., and Lordet, F., "Vibrational Nonequilibrium in a Supersonic Expansion with Reactions: Application to O_2–O," *Journal of Chemical Physics*, Vol. 104, No. 10, 1996, pp. 3579–3597.